Structural properties of gold clusters at different temperatures

M.A. Mahladisa*, L. Ackermann* and P.E. Ngoepe*†

A series of gold clusters consisting of aggregates of from 13 to 147 atoms was studied using the Sutton–Chen type many-body potential in molecular dynamics simulations. The properties of these clusters at temperatures from 10 K to 1000 K were investigated in terms of their energy content and their respective radial distribution functions, to describe their melting behaviour. The larger clusters were deduced to melt over a range of temperatures rather than to undergo a distinctive phase change at a specific temperature as in the bulk material.

Introduction

The structural, electronic, optical, thermodynamic, spectroscopic, magnetic, and chemical properties of isolated clusters of atoms and their assemblies possess properties that differ from those of the bulk material.[1–5] Metal nanoclusters containing a few atoms show quantum size effects which give them unique attributes and make them interesting candidates for the building blocks of nanostructured materials and nanoelectronic digital circuits.[1] Metallic clusters provide a challenging subject of study because they are intermediate between isolated atoms and molecules, at the one extreme, and bulk solids at the other, they have a large surface to volume ratio, and they often exhibit a novel phenomenology.[6,7] In general, clusters have higher magnetic moments than the corresponding bulk material, which is due mainly to reduced atomic coordination and corresponding reduced valence band width.[7]

Gold is specially relevant for both fundamental and applied research. In its chemical and physical properties in the bulk form, it is the most inert and softest metal in relation to its cohesive energy.[8] Apart from its commercial value, the unique chemical and physical properties offered by gold are increasingly being investigated in a growing number of applications. These include uses within the fields of nanotechnology and medicine for products such as smart cards, automotive electronics, sensors, medical implants and drug delivery systems.

Gold clusters provide special benefits when supported on metal oxides such as TiO_2 to form Au/TiO_2 catalysts. The metal shows extraordinarily high activity for low-temperature catalytic combustion, partial oxidation of hydrocarbons, hydrogenation of unsaturated hydrocarbons, and reduction of nitrogen oxides.[9] Gold clusters promote the reaction between CO and O_2 to form CO_2 at temperatures as low as 40 K.[5,9,10] This activity depends on the size of the cluster; when the catalyst is too small or too big, it becomes less effective. There is a certain size range for the clusters to work optimally. Valden *et al.*[9] found that the Au/TiO_2 catalyst is effective when the diameter of the cluster is about 3.5 nm. The catalytic activity may be attributed to the properties of the metal/support interface, the presence of ionic gold or to atoms with unsaturated coordination in small gold clusters.

*Materials Modelling Centre, Department of Physics, School of Physical and Mineral Sciences, University of Limpopo‡, Sovenga 0727, South Africa; and Manufacturing and Materials Technology, CSIR, P.O. Box 395, Pretoria 0001.
†Author for correspondence. E-mail: ngoepep@ul.ac.za
‡The former University of the North.

We are interested in finding the stable structures of these small materials as clusters are known to be unstable even at low temperatures.[1,11] Michaelin *et al.*[1] found that Au nanoclusters, between 19 and 75 atoms in size, are disordered even in their lowest-energy configuration. Small clusters appeared to be amorphous instead of crystalline or quasicrystalline. Gold clusters adopt different forms, some based preferentially on icosahedra, some in decahedral form.[1,3]

Another aspect of interest is the melting point of nanoclusters and their resistance to high temperatures. Nanomaterials are less stable and have lower melting points than the respective bulk materials.[12–19] Buffat and Borel[12] and Rodriguez-Lopez *et al.*[7] studied the effect of size on the melting of gold particles and found the temperature of melting fell as the particle size became smaller.[1,13,14] The size of the particle thus plays a vital role in the stability and melting of a particular material. Nakamura *et al.*[13] reported that cluster orientation also plays a role in its stability. Doye and Wales[14] built assemblies of different shapes and found that the zigzag structure is more stable than those that are linear and rectangular. The lower melting point in clusters is attributed to the higher proportion of surface atoms than present in larger particles. Surface atoms have fewer nearest neighbours and are more weakly bound and less constrained in their thermal motion than atoms in the body of a material.[19]

This paper presents molecular dynamics simulations to describe the properties of clusters. The stability of different clusters under various thermodynamic conditions was considered and served as a basis for analysing melting behaviour in terms of cluster size. Where possible, results are compared with what has been reported in literature. It is hard, however, to determine the exact melting points of the clusters because of their different properties from the bulk. For example, the energy–temperature plot for the clusters does not show a jump that signifies a distinctive solid–liquid transition as in the bulk. Furthermore, clusters do not readily allow calculations at constant pressure, which is a preferred condition under which to determine the temperature of melting.

Methods

Molecular dynamics (MD)[20–23] simulations were carried out under constant-energy conditions for gold clusters ranging in size between 13 and 147 atoms. Molecular dynamics in general solves classical equations of motion (Newton's equations) for a set of molecules. This approach requires a forcefield or interatomic potential to perform calculations on atomic systems. The simulations were carried out using an academic code (DL-POLY).

This work makes use of a many-body Sutton–Chen (SC) potential,[14,24–29] which is of proven efficiency for the purpose. The SC (energy) potential has the form:

$$E_{\text{tot}} = \varepsilon \sum_i \left[\tfrac{1}{2} \sum_{i \neq j} \left(\frac{a}{r_{ij}} \right)^n - C \sqrt{\sum_{i \neq j} \left(\frac{a}{r_{ij}} \right)^m} \right], \qquad (1)$$

where r_{ij} is the separation between atoms i and j, C is a dimensionless parameter, ε is a parameter with the dimensions of energy, a has the dimensions of length, and n and m are positive integers. The parameters ε, C and a are not independent and are determined by the equilibrium lattice parameters and lattice energy of a face-centred lattice (fcc). The exponents n and m are assigned for modelling different metals by fitting the elastic constants as closely as possible. For a given crystal structure, the Sutton–Chen potential is defined by n and m. This is because the equilibrium condition for a particular crystal

structure fixes the parameter *C*. If two metals, with the same crystal structure, may be represented by the same values of *n* and *m*, then the results obtained for one metal may be directly converted into the results of another simply by rescaling the units of energy and length. The Sutton–Chen potential, which takes the form of the Finnis–Sinclair[30] potential, can be interpreted as being similar to the embedded atom potentials,[31] but with a rather different embedding function which gives a different form to the many-body term. A difference that may be important to the description of surfaces is that the many-body term falls off more slowly with distance. Sutton and Chen[24] gave various parameter values to different metals; those used in our calculations are based on the ones for gold, but slightly modified to obtain a closer match with experimental data.[29]

The numbers of atoms in the gold clusters investigated were 13 (cube–octahedra), 13 (icosahedra), 19, 38, 55 and 147. This selection over a range of cluster sizes allowed the study of cluster properties as a function of cluster geometry and, in particular, of the number of atomic layers. Molecular dynamics simulations were performed under constant-energy conditions for 60 000 MD steps at different temperatures (time step 5 fs; equilibration after 20 000 steps). This allowed an analysis of the typical structural processes during melting. The Verlet algorithm, which uses the positions and accelerations at time *t*, and the positions from the previous step, $r(t - \delta t)$, to calculate the new positions at $(t + \delta)$, $r(t + \delta t)$, was used to integrate the equations of motion.

Various properties were calculated during the simulations. The total energy and the radial distribution function (RDF), reported for various clusters, are all well stabilized with respect to the sampling (number of steps in the production run). The radial distribution functions describe the structure at different temperatures and can be used to study the melting behaviour for various solid systems.[21,23,29,32] They also predict the mobility of atoms in the system and can be used to differentiate between solid, liquid and gas phases. The structures of the different gold clusters investigated are illustrated in Figs 1a–f.

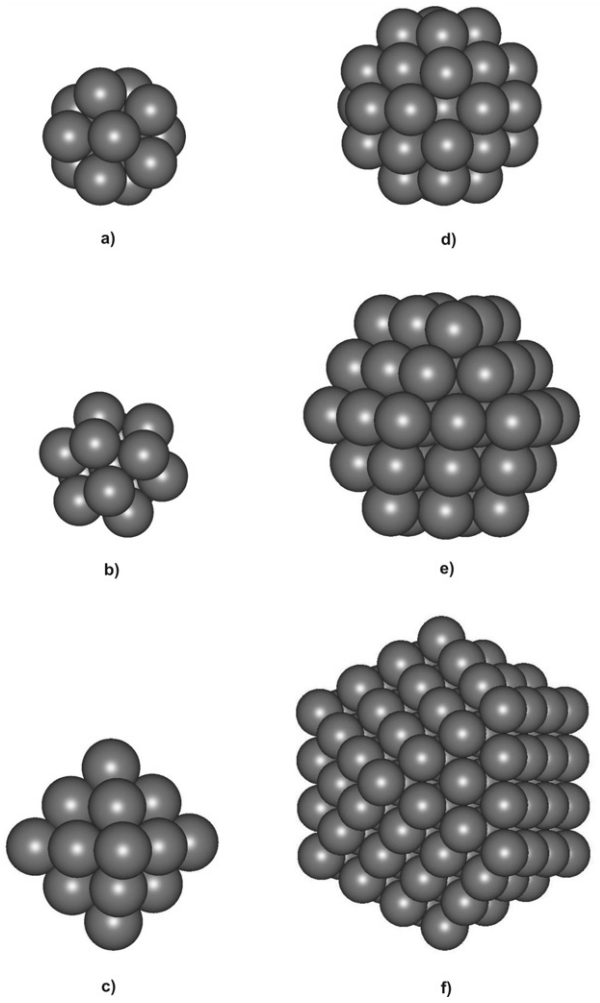

Fig. 1. Model clusters of (**a**) Au_{13} (I_h), (**b**) Au_{13} (O_h), (**c**) Au_{19}, (**d**) Au_{38}, (**e**) Au_{55} and (**f**) Au_{147}.

Results and discussion

Modelling the melting process

Figure 2 shows the total (Sutton–Chen) energy per atom for a series of clusters at different temperatures. The energy–temperature plots do not show a clear discontinuity (transition between a solid and a liquid phase) as in the bulk. Rodriguez-Lopez *et al.*[7] and Wang *et al.*[33] show in their cluster calculations that there is a jump in the potential energy, corresponding to the melting of the clusters. They report a melting temperature that fell with decrease in the cluster size. In our calculations, melting in the clusters was not clearly detectable from the energy–temperature plots. Figure 2 shows that the Au_{13} cluster has higher energies than Au_{19} at all temperatures. The figure also indicates that the total energies of the Au_{38} and Au_{55} clusters are lower than those for Au_{13} and Au_{19}. The plots show instabilities above a temperature as low as 100 K.

Figure 2 implies that the cluster with fewer atoms will be less stable than one with more, meaning that the smaller clusters will melt before bigger assemblages with increasing temperature. Similarly, Fig. 3 shows that cluster stability increases with the number of atoms in the cluster.

Structural changes and radial distribution functions

The sizes of clusters investigated in this study were chosen to allow for highly symmetric geometries of closed shells of atoms. With growing cluster size, this led to aggregates with layered (onion-like) structures. One therefore expects the equilibrium geometries of clusters to follow cube–octahedral or icosahedral construction principles, at least at low temperatures. Indeed, comparison of these structural variants (e.g. for Au_{13} or Au_{55}) is one of the objectives of this study. If, as here, elevated temperatures are considered, the barriers between these limiting (high symmetry) cases may well start to disappear, as the cluster structure becomes progressively less ordered.

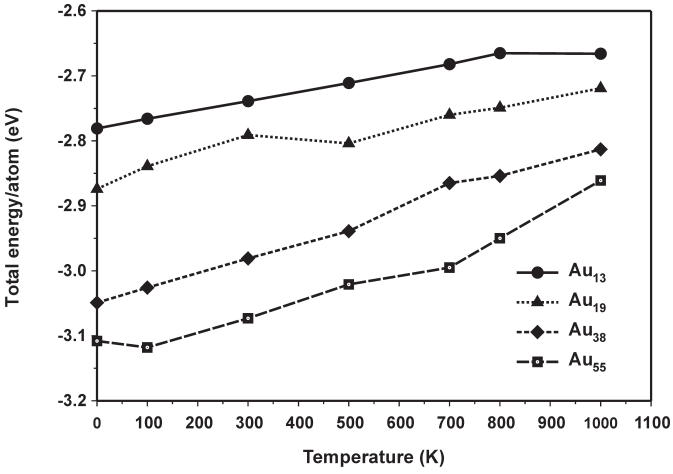

Fig. 2. Binding energy per atom versus temperatures for Au_{13}, Au_{19}, Au_{38} and Au_{55} clusters.

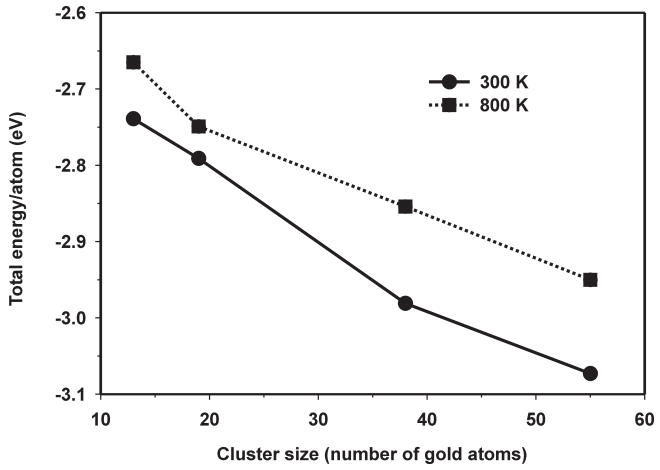

Fig. 3. Binding energy per atom as a function of cluster size at 300 K and 800 K.

To monitor structural changes in these clusters, one needs a probe that permits the analysis of such features in terms of their layering. Here the radial distribution function, readily available from the MD calculations, proves useful. The RDF concisely characterizes the average structural environment of the atoms, reflecting the degree of order in the cluster. This means that one can expect quite different RDF plots, depending on the number of atom shells. Moreover, for any given cluster size, the RDF will give an indication of melting behaviour. Figure 4 compares the RDFs of clusters as a function of cluster size corresponding to a temperature of 300 K, where the structures are expected to be largely solid.

While the peak found at lowest r value (≈2.7 Å) for each of these clusters corresponds to the nearest-neighbour distance between Au atoms, the peaks corresponding to larger radii are due to gold atoms which are not adjacent to each other. Clearly, the relative importance of those nearest-neighbour distances is greater in smaller clusters, being represented by a pronounced peak at the nearest-neighbour distance.

The smallest cluster (n = 13), consisting of a central atom and one shell of surrounding atoms, shows only two discernible peaks (a third, very small one at 5.4 Å is found at low temperatures, corresponding roughly to the largest inter-atomic distance across the cluster, that is, twice the Au–Au bond distance). The first reflects the Au–Au distances between the central atom and atoms of the first shell as well as inter-atomic distances within the surrounding shell. While these distances are identical in the case of a cube–octahedron, they differ slightly in the alternative ideal case, that of an icosahedron. The RDF plot for the cube–octahedron (Au_{13}), depicted in Fig. 4, did not show any significant differences from the latter (not shown). This could be seen as an indication that at 300 K both structures are sampled in an MD run of this length, where both are of closely similar energy and the energy barrier between them is not significant.

The second peak in the RDF of Au_{13} is a superposition of two Au–Au distances that obtains between pairs of atoms of the outer shell of this cluster and can therefore be attributed to this shell. For larger clusters, identifying other peaks with additional shells is not simple (see below).

For Au_{19}, Au_{55} and Au_{147} an increase in complexity of the corresponding RDF plots was observed. Unmistakably, these nanoclusters are all highly ordered, as indicated by the shape of the additional peaks. In a cluster like Au_{147}, the shape of the RDF plot indicates the prevalence of certain inter-atomic distances (related to those present in fcc metals, since the cluster can be seen as a fragment of such a crystal). It is not possible, however, to relate the number of peaks seen in the RDF to the cluster architecture in a simple way, nor to the number of shells involved. Nevertheless, the RDF is a useful tool to characterize different gold clusters and to monitor certain geometry-related features.

RDFs of melting clusters

The RDF of a typical gold cluster changes significantly in various respects, depending on the simulation temperature. Figure 5 depicts a series of such plots for Au_{55}.

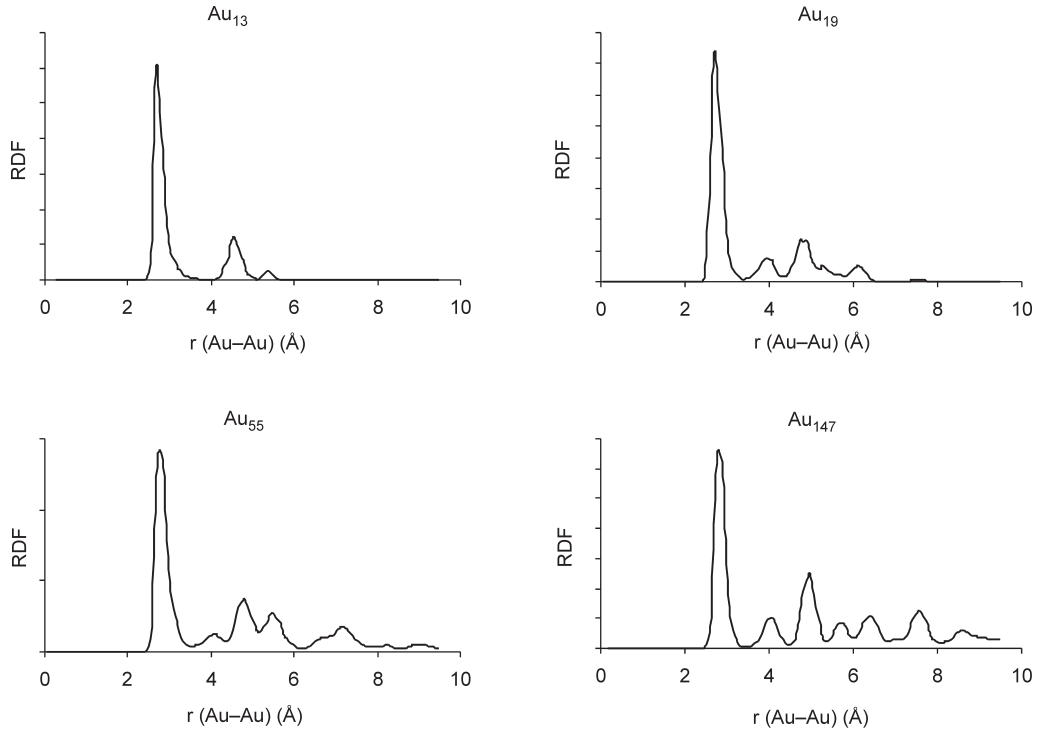

Fig. 4. Radial distribution function at 300 K for gold clusters of different sizes (13, 19, 55 and 147 atoms).

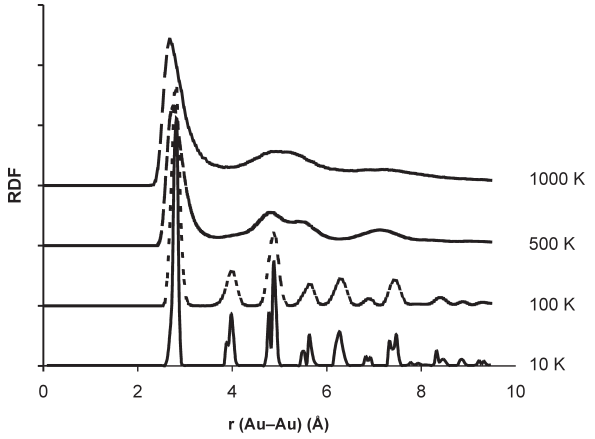

Fig. 5. Radial distribution function of Au_{55} at different temperatures.

At the lowest temperature considered (10 K), one observes rather sharp and well-separated peaks. The peak positions corresponding to a temperature of 100 K were identical but were noticeably broadened and some merged.

At an even higher temperature (500 K), the only peak that remains clearly distinguishable is the one corresponding to the smallest r (≈2.7 Å), representing the average nearest-neighbour Au–Au distance. All other peaks are similarly broadened.

At 1000 K the RDF plot assumes the characteristic shape of a typical fluid function. Comparisons with other simulations at 1200 K and 2000 K show that no significant changes take place above this temperature.

It follows that the RDF can be used to monitor the melting process. However, it is difficult to reduce the temperature intervals around melting for the clusters considered on the basis of the RDF only. At a temperature of 500 K, where the RDF of Au_{55} is still clearly different (more structured) from that of the molten cluster (at 1000 K), the plot for radii above $r = 3$ Å becomes so featureless that one can hardly speak of a solid any more. It is in this intermediate temperature region that the energy curves shown in Fig. 2, for example, show a peculiar behaviour. So instead of marking a single, sharp phase transition, the RDFs shown here rather suggest a process of pre-melting (surface melting) and subsequent, progressive melting of the cluster with rise in temperature. To corroborate this explanation, the energy plots were analysed in more detail. In calculations using a higher resolution of the simulation temperatures reported here, we did indeed observe several transitions for most of the clusters discussed in this work.

Conclusions

Molecular dynamics has been used as the basis of energy calculations on gold clusters of different sizes at different temperatures. From these simulations, gold clusters proved to have melting temperatures that are lower than the bulk gold. We also demonstrated that the clusters become more stable as the number of atoms in the clusters increases. This work forms a foundation for the study of gold nanowires, which are extensively studied throughout the world in view of their important applications in nanotechnology.[33]

We thank Mintek (through the AuTEK project) and the NRF/Royal Society collaboration for financial support.

1. Michaelin K., Rendon N. and Garzon I.L. (1999). Structure and energetics of Ni, Ag, and Au nanoclusters. *Phys. Rev. B* **60**, 2000–2010.
2. Luedtke W.D. and Landman U. (1996). Structure, dynamics, and thermodynamics of passivated gold nanocrystallites and their assemblies. *Phys. Chem.* **100**, 13323–13329.
3. Bilalbegovic B. (58). Structure and stability of finite gold nanowires. *Phys. Rev. B* **58**, 15412–154415.
4. Zhao J., Yang J. and Hou J.G. (2003). Theoretical study of small two-dimensional gold clusters. *Phys. Rev. B* **67**, 085404-1-085404-4.
5. Goodman D.W. (2004). Catalysis by supported gold nanoclusters. *Dekker Encyclopedia of Nanoscience and Nanotechnology,* 611–620.
6. Rogan J., Ramirez R., Romero A.H. and Kiwi M. (2003). Rearrangement collisions between gold clusters. *Eur. Phys. J. D* 1–10.
7. Rodriguez-Lopez J.L., Montejano-Carrizales J.M. and Jose-Yacaman M. (2003). Molecular dynamics study of bimetaliic nanoparticles: the case of Au_xCu_y alloy clusters. *Appl. Surf. Sci.* **219**, 56–63.
8. Soler J.M., Garzon I.L. and Joannopoulos J.D. (2001). Structural patterns of unsupported gold clusters. *Sol. State Commun.* **117**, 621–625.
9. Valden M., Lai X. and Goodman D.W. (1998). Onset of catalytic activity of gold clusters on titania with the appearance of nonmetallic properties. *Science* **281**, 1647.
10. Haruta M. and Date M. (2000). Advances in the catalysis of Au nanoparticles. *Appl. Cat. A: General* **222**, 427–437.
11. Garzon I.L., Michaelin K., Beltran M.R., Posada-Amarillas A., Ordejon P., Artacho E., Sanchez-Portal D. and Soler J.M. (1998). Lowest energy structures of gold nanoclusters. *Phys. Rev. Lett.* **81**, 1600–1603.
12. Buffat Ph. and Borel J-P. (1976). Size effect on the melting temperature of gold particles. *Phys. Rev. A* **13**, 2287–2298.
13. Nakamura J., Kobayashi N. and Aono M. (2001). Electronic states and structural stability of gold nanowires. *Rirken Rev.* **37**, 17–20.
14. Doye J.P.K. and Wales D.J. (1998). Global minima for transition metal clusters described by Sutton–Chen potentials. *New J. Chem.*, 733–744.
15. Cleveland C.L., Luedtke W.D. and Landman U. (1998). Melting of gold clusters: Icosahedral precursors. *Phys. Rev. Lett.* **81**, 2036–2039.
16. Cleveland C.L., Luedtke W.D. and Landman U. (1999). Melting of gold clusters. *Phys. Rev. B*, **60**, 5065–5075.
17. Kusche R., Hippler Th., Schmidt M., von Isserndorff B. and Haberland H. (1999). Melting of free sodium clusters. *Eur. Phys. J. D*, **9**, 1–4.
18. Cortie M.B. and van der Lingen E. (2002). Catalytic gold nano-particles. *Mater. Forum* **26**, 1–4.
19. Schmidt M., Kusche R., von Issendorf B. and Haberland H. (1998). Irregular variations in the melting point of size-selected atomic clusters. *Nature* **393**, 238–240.
20. Allen M.P. and Tildesley D.J. (1987). *Computer Simulation of Liquids.* Oxford University Press, Oxford.
21. Leach A.R. (1996). *Molecular Modelling: Principles and Applications.* Addison Wesley Longman, Singapore.
22. Grant G.H. and Richards W.G. (1995). *Computational Chemistry.* Oxford University Press, Oxford.
23. Atkins P.W. (1998). *Physical Chemistry,* 6th edn. Oxford University Press, Oxford.
24. Sutton A.P. and Chen J. (1990). Long-range Finnis–Sinclair potentials. *Phil. Mag. Lett.* **61**, 139–146.
25. Todd B.D. and Lyndell-Bell R.M. (1993). Surface and bulk properties of metals modelled with Sutton–Chen potentials. *Surf. Sci.* **281**, 191–206.
26. Lyndell-Bell R.M. (1991). Migration of adatoms on the (100) surface of face-centred-cubic metals. *Surf. Sci.* **259**, 129–138.
27. Liem S.Y. and Yu Chan K. (1995). Simulation study of platinum adsorption on graphite using the Sutton–Chen potential. *Surf. Sci.* **328**, 119–128.
28. Wen Wu G. and Yu Chan K. (1996). Morphology of platinum clusters on graphite at different loadings. *Surf. Sci.* **365**, 38–52.
29. Mahladisa M.A. (2004). *Computer simulation studies of bulk and surface properties of gold.* M.Sc. thesis, University of the North, Sovenga.
30. Finnis M.W. and Sinclair J.E. (1984). A simple empirical N-body potential for transition metals. *Phil. Mag. A* **50**, 45–55.
31. Daw M.S. and Baskes, M.I. (1984). Embeded-atom method: derivation and application to impurities, surfaces and other defects in metals. *Phys. Rev. B* **29**, 6443–6452.
32. Holender J.M. (1990). Molecular-dynamics studies of the thermal properties of the solid and liquid fcc metals Ag, Au, Cu, and Ni using many-body interaction. *Phys. Rev. B,* **41**, 8054–8061.
33. Wang Y., Teitel S. and Dellago C. (2004). Melting and equilibrium shape of icosahedral gold nanoparticles. *Chem. Phys. Lett.* **394**, 257–261.